

Work relation for determining the mixing free energy of small-scale mixtures

Akira Yoshida* and Naoko Nakagawa†

Department of Physics, Ibaraki University, Mito 310-8512, Japan

(Dated: November 12, 2021)

In thermodynamically characterizing a mixture comprising a finite number of molecules, we consider two kinds of alchemical protocol for producing a mixture from a pure substance. The first is a simple alchemical protocol, whereas the second is a protocol comprising a series of processes with feedback control and mixing with semipermeable membranes. A comparison of the two numerically determined free-energy changes provides a combinatorial factor that indicates the indistinguishability of the molecules. The comparison also uncovers a work relation for determining the mixing free energy, which generates the basic properties of mixtures. We demonstrate a numerical calculation of applying the work relation to a mixture of argon and krypton. The mixing free energy clearly shows the characteristics of liquid–vapor transition.

I. INTRODUCTION

Solutions exhibit a variety of fascinating phenomena. Various combinations of solutes and solvents have been explored to create properties useful in scientific and industrial applications. Free energy and entropy are central quantities that characterize the properties of solutions [1, 2]. Thermodynamic measurements have been performed intensively to quantitatively determine these quantities, and the accumulated results have been integrated into a huge database [3]. The thermodynamic measurement of small-scale solutions is in its early stage of development [4–7] although recent micro-manipulation techniques have shed light on the non-triviality of small scales, including the anomalous diffusion of macromolecules and stabilization of protein folding by aggregation [8–11]. In cell sciences, liquid–liquid phase separation with the coexistence of dilute and concentrated solutions has been intensively studied from the viewpoint of biological functions [12–17]. Thermodynamic quantification is necessary to understand such interesting phenomena. Numerical experiments may be powerful for the study of small systems. This paper thus proposes an effective numerical method for the thermodynamic measurement of small-scale solutions.

The thermodynamics of small systems was proposed in the 1960’s on the basis of statistical mechanics [18]. In the past two decades, stochastic thermodynamics has been studied intensively, aiming for a physical understanding of molecular machines [19–22]. Furthermore, information thermodynamics has been formulated by combining stochastic thermodynamics and information theory [23, 24], allowing us to approach biological phenomena from the perspective of information processing [25].

We now address free energy. Several methods have been and are being developed for the numerical calculation of free energy [26, 27]. The change in free energy in stochastic thermodynamics has been formulated

as the Jarzynski or Crooks work relation consistently with the second law of thermodynamics [21, 22]. Using these relations, the change in free energy for the binding of biomolecules is determined by micro-manipulation [28, 29].

Alchemical free energy calculations is applicable to molecular dynamics simulation [30, 31] and is often used in drug discovery [32–37]. The change in free energy is measured from the work required to substitute some parts of a large molecule alchemically; i.e., by changing microscopic parameters of the molecule. If microscopic operations are allowed, we may realize alchemy from one substance to another, or create a solution from a pure substance. We then ask if the work relations are applicable to such alchemical protocols. We face two problems. The first is the indistinguishability of molecules. To create a solution alchemically, many molecules should be manipulated at once; however, the usual alchemical method is designed for a single molecule and the indistinguishability is not considered. The second problem is the quantity accessible using the alchemical method. The important quantity is the mixing free energy rather than the free energy for solutions.

The mixing free energy, which involves excess chemical potentials or activity coefficients, corresponds to the work required for quasistatic mixing. It determines properties of a solution, such as equilibrium constants and solubility. However, theories for estimating the mixing free energy are limited to rather dilute solutions [38–40]. A simpler numerical method applicable to the general concentration and valid regardless of the system size would be valuable. We thus propose a method for molecular dynamics simulations that estimates the mixing entropy of finite-size systems by combining the alchemical method with stochastic thermodynamics and information thermodynamics.

This paper is organized as follows. In Sec. II, we describe the setup of the system that we consider and formulate the work required to perform external operations on the system. In Sec. III, work relations that connect the work to the free-energy change are briefly reviewed. We then address the problem of the conventional work relations when they are applied to alchemical

* a.yoshida.phys@gmail.com

† naoko.nakagawa.phys@vc.ibaraki.ac.jp

processes and propose (9) as an alternative work relation. To examine the proposition, we introduce two candidate protocols that determine the free energy of solutions in Sec. IV. Comparing the numerically determined free energies for the two protocols clarifies (21) and (22), which lead to combinatorial factor. In Sec. V and Sec. VI, we investigate a work relation for the mixing Gibbs free energy. We first deal with an isotope mixture and formulate a work relation in Sec. V. We then extend the formula to general mixtures and propose (40), which is estimated as (41) or (43), in Sec. VI. Using (43) in a molecular dynamics simulation, we determine the mixing Gibbs free energy for a mixture of argon and krypton in Sec. VII. The obtained mixing free energy clearly shows the characteristics of the liquid–vapor transition. Section VIII is devoted to concluding remarks. All details of the model and the protocols for numerical examination are described in Appendices A and B. The numerically determined free energies are examined carefully in Appendices C and D. Appendix E compares our results with those of statistical mechanics. Parameters for the numerical experiments in Sec. VII are specified in Appendix F.

II. SETUP

We deal with classical systems of N molecules packed in a rectangle container of volume V . The container may be spatially partitioned by walls or semipermeable membranes. The walls or membranes are rigid and transparent to heat and their positions do not fluctuate. The surrounding environment is at a constant temperature T . For simplicity, we limit the type of molecule to be monoatomic in this paper, but our proposed methods can be extended to more general molecules as discussed in Sec. VIII. We write the Hamiltonian of the system as

$$H(\Gamma; \alpha) = \sum_{i=1}^N \frac{\mathbf{p}_i^2}{2m_i} + \Phi(\{\mathbf{r}_i\}; \alpha_\Phi), \quad (1)$$

where $\Gamma = (\{\mathbf{r}_i\}, \{\mathbf{p}_i\})$ with the position \mathbf{r}_i and momentum \mathbf{p}_i for the i th molecule, and $(\{a_i\})$ is an abbreviation of (a_1, a_2, \dots, a_N) . m_i is the mass of the i th molecule and the potential Φ comprises the interaction among molecules and the interaction between molecules and walls or membranes of the container, which are parameterized by the set α_Φ . α is the set of parameters in the Hamiltonian, $\alpha = (\{m_i\}, \alpha_\Phi)$. See Appendix A for an example of α and $H(\Gamma; \alpha)$.

Suppose that an external operator changes the value of α in the period $0 \leq t \leq \tau$. For a protocol $\dot{\alpha} = (\alpha(t))_{t \in [0, \tau]}$, where $\alpha_0 = \alpha(0)$ and $\alpha_1 = \alpha(\tau)$, the work done by the external operator is written as

$$\hat{W}(\hat{\Gamma}) = \int_0^\tau ds \frac{d\alpha}{ds} \cdot \frac{\partial H(\Gamma(s); \alpha)}{\partial \alpha} \Big|_{\alpha=\alpha(s)}. \quad (2)$$

where $\hat{\Gamma} = (\Gamma(t))_{t \in [0, \tau]}$ is a trajectory in the phase space.

We assume below that the system is in equilibrium at α_0 for $t \leq 0$.

III. PROBLEMS OF THE WORK RELATION IN MICROSCOPIC OPERATIONS

We first consider macroscopic operations such as changing the volume of the container and the positions of membranes. Thermodynamic work corresponds to an ensemble average of the work over trajectories $\hat{\Gamma}$, which we write as $\langle \hat{W} \rangle$. The difference in the Helmholtz free energy satisfies

$$\Delta F \leq \langle \hat{W} \rangle, \quad (3)$$

where $\Delta F = F(T, \alpha_1, N) - F(T, \alpha_0, N)$. The equality holds in the quasistatic limit $\tau \rightarrow \infty$. The work relation (3) is reformulated as the Jarzynski equality [21]

$$\Delta F = -k_B T \log \langle e^{-\beta \hat{W}} \rangle, \quad (4)$$

where $\beta = (k_B T)^{-1}$ with the Boltzmann constant k_B . With (4), the free energy becomes measurable in mesoscopic systems of finite N applicable to single-molecule manipulations, and moreover, the free-energy change can be identified from finite speed operations regardless of whether the system reaches equilibrium at $t = \tau$.

We next consider microscopic operations called alchemical processes, which changes the attributes of molecules, such as the mass and size. Alchemical methods are usually used to estimate the effect of substituting some groups into a large single molecule [30, 31]. We note that an alchemical method itself is not necessarily limited to single molecules but can be applied to multi-molecule systems so as to create a mixture from a pure substance. Our first question is then whether the work relation (4) can be used in determining the Helmholtz free energy of the mixture created from the pure substance.

The important quantity that determines the thermodynamic properties for the mixture is not the free-energy difference between the mixture and the pure substance but the mixing free energy $\Delta_{\text{mix}}G$. This corresponds to the work required for quasistatic mixing at constant temperature and constant pressure, which is the sum of the mixing entropy $\Delta_{\text{mix}}S$ and the enthalpy change in mixing. The mixing free energy gives the equilibrium constant and can be used as a variation function with which to identify the equilibrium state through its minimization. We then ask the second question of whether there exists a work relation that can be used to determine $\Delta_{\text{mix}}G$.

IV. WORK RELATION FOR MICROSCOPIC OPERATIONS

We consider a mixture of two species A and B, whose numbers of molecules are n and $N - n$, respectively.

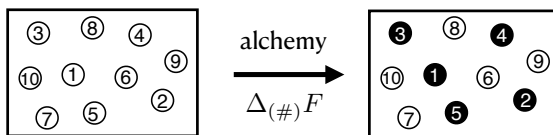


FIG. 1. Schematic figure of the alchemical process for creating the mixture of distinguished molecules to determine $\Delta_{(\#)}F$ in (7).

We write the Helmholtz free energy for a pure substance of A as $F_A(T, V, N)$ and that for the mixture as $F_{AB}(T, V, n, N - n)$. To answer the first question, we focus on the free-energy difference between these two

$$\Delta F \equiv F_{AB}(T, V, n, N - n) - F_A(T, V, N), \quad (5)$$

and ask what is the work relation that can be used to obtain ΔF in the alchemical process.

We put N molecules of species A in a container and index all N molecules in order; i.e., $i = 1, 2, \dots, N$. After relaxing the system to equilibrium, we change the attributes of the first n molecules, $1 \leq i \leq n$, alchemically as they become another species B as depicted in Fig. 1. The resulting system is similar to a typical two-component mixture except that all molecules are indexed. We call the molecules a distinguished mixture. Although real molecules are never indexed, the present procedure may be useful in numerical experiments.

We write the work for completing the alchemical process as $\hat{W}_{(\#)}(\hat{\Gamma})$. Applying (4), we can determine the free energy $F_{AB\#}(T, V, n, N - n)$ for the distinguished mixture of A and B as

$$\Delta_{(\#)}F \equiv F_{AB\#}(T, V, n, N - n) - F_A(T, V, N), \quad (6)$$

$$\Delta_{(\#)}F = -k_B T \log \langle e^{-\beta \hat{W}_{(\#)}} \rangle. \quad (7)$$

In the subsection below, we show numerically that $\Delta F \neq \Delta_{(\#)}F$; i.e.,

$$F_{AB}(T, V, n, N - n) \neq F_{AB\#}(T, V, n, N - n), \quad (8)$$

which means that the alchemical process in Fig. 1 does not provide the free energy for the mixture. From the thermodynamic argument in the following subsections with numerical examinations, we conclude that the formula that gives the true free-energy change (5) is

$$\Delta F = -k_B T \log \left[\frac{N!}{n!(N - n)!} \langle e^{-\beta \hat{W}_{(\#)}} \rangle \right], \quad (9)$$

which we propose as the Jarzynski work relation valid for general alchemical processes. In the quasistatic limit, (9) is written as

$$\Delta F = \langle \hat{W}_{(\#)} \rangle - k_B T \log \left[\frac{N!}{n!(N - n)!} \right]. \quad (10)$$

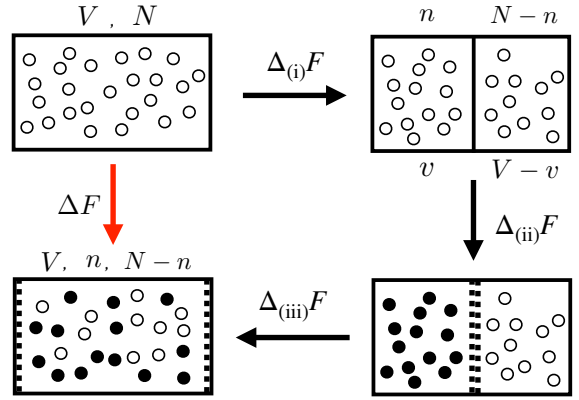


FIG. 2. Operation protocol for obtaining F_{AB} by thermodynamic processes (i), (ii), and (iii). Refer to Table I for a summary of respective processes. The red arrow indicates not an experimental protocol but a difference between a pure substance A and a mixture of A and B. Process (i) requires a feedback control to fix the number n of molecules in the right chamber.

To show (9), we design a protocol comprising three processes as schematically illustrated by the three black arrows in Fig. 2 and summarized in Table I. Process (i) is the insertion of a wall partition that divides the container into two. This insertion is performed under feedback control as explained in Sec. IV A, and the corresponding work relation is therefore given by information thermodynamics [23, 24]. In process (ii), we change the species of all molecules in the left chamber and replace the wall partition with two ideal semi-permeable membranes. We then shift each semi-permeable membrane to mix the two substances in process (iii). We specify respective formulas of the work relation in Sec. IV B and Sec. IV C.

With these respective formulas, we numerically determine the respective free-energy changes $\Delta_{(i)}F$, $\Delta_{(ii)}F$ and $\Delta_{(iii)}F$. The total change should be ΔF in (5):

$$\Delta F = \Delta_{(i)}F + \Delta_{(ii)}F + \Delta_{(iii)}F. \quad (11)$$

The right-hand side of (11) is thermodynamically definite without the difficulty of the distinguishability of molecules. In Sec. IV E, we compare ΔF with the alchemical free-energy change $F_{AB\#} - F_A$ determined according to (7), which concludes the validity of (9) within numerical error.

A. Formula for $\Delta_{(i)}F$

In process (i), we spontaneously partition the container into two by inserting a rigid wall with a negligible thickness, where the volumes of the left and right chambers are v and $V - v$. Let Γ be the microstate at the time of

process	operation	ΔF
(i)	partition with feedback control	$F_A(T, v, n) + F_A(T, V - v, N - n) - F_A(T, V, N)$
(ii)	alchemy the left side molecules	$F_B(T, v, n) - F_A(T, v, n)$
(iii)	mix by shifting the membranes	$F_{AB}(T, V, n, N - n) - F_A(T, V - v, N - n) - F_B(T, v, n)$
(#)	alchemy the molecules $1 \leq i \leq n$	$F_{AB\#}(T, V, n, N - n) - F_A(T, v, n)$

TABLE I. Summary of processes schematically illustrated in Figs. 1 and 2. We use the subscripts A, B, and AB to specify the quantities for the pure substance A, the pure substance B, and their mixture, respectively.

partitioning and $n_v(\Gamma)$ be the number of molecules in the left chamber of volume v . The probability distribution $\rho_v(n)$ for the number n of molecules in the left chamber is written as

$$\rho_v(n; T, V, N) = \int d\Gamma \delta_{n_v(\Gamma), n} \rho_{\text{eq}}(\Gamma), \quad (12)$$

where $\rho_{\text{eq}}(\Gamma)$ is the canonical distribution before the partition.

We perform feedback control to insert a wall only when $n_v(\Gamma) = n$. The work required for the spontaneous insertion depends on Γ , which we write as $\hat{W}_{(i)}(\Gamma)$. The change in the free energy satisfies

$$e^{-\beta \Delta_{(i)} F} = \int d\Gamma \delta_{n_v(\Gamma), n} e^{-\beta \hat{W}_{(i)}(\Gamma)} \rho_{\text{eq}}(\Gamma), \quad (13)$$

where $\delta_{i,j}$ is the Kronecker delta. The relation (13) is a version of the Jarzynski work relation putting $\delta_{n_v(\Gamma), n}$ in the integral because we perform the work only when $n = n_v(\Gamma)$. (13) belongs to the generalized Jarzynski relation derived in information thermodynamics, which is formulated for general feedback controls [23].

We design the interaction between the inserted wall and each molecule such that

$$\hat{W}_{(i)}(\Gamma) = 0. \quad (14)$$

This can be satisfied when each molecule acts as a point of mass with respect to the inserted wall. We choose this particular setting because ΔF , which is a quantity to be determined, is independent of the properties of the inserted wall.

Substituting (14) into the relation, we obtain

$$\Delta_{(i)} F = -k_B T \log \rho_v(n; T, V, N). \quad (15)$$

Hereafter, we abbreviate $\rho_v(n; T, V, N)$ as $\rho_v(n)$. The validity of (15) is examined from the perspective of statistical mechanics in Appendix E. We are now able to determine $\Delta_{(i)} F$ without performing the insertion. One should simply count the number of molecules in the region corresponding to the left chamber from time to time and determine $\rho_v(n)$.

Note that the protocol (i) is common regardless of the species of the initial pure substance or the composition of the final mixture. $\Delta_{(i)} F$ is expressed by a general form with an error of $o(\log N)$. See (27) and Appendix C.

B. Work relation for $\Delta_{(ii)} F$

We next consider $\Delta_{(ii)} F$, which corresponds to the difference between two pure substances as

$$\Delta_{(ii)} F = F_B(T, v, n) - F_A(T, v, n), \quad (16)$$

where F_B is the Helmholtz free energy for the substance B. We apply an alchemical process to determine $\Delta_{(ii)} F$. We change all molecules in the left chamber to other species according to the same protocol. We emphasize that we do not need to consider whether process (ii) is a microscopic or macroscopic operation because all molecules in the left chamber are changed in the same manner. We add that there are several numerical ways to determine $\Delta_{(ii)} F$, and that the values of F_A and F_B may be referenced from a database [3].

The alchemical process (ii) is expressed by the change in the Hamiltonian, and we thus define the required work $\hat{W}_{(ii)}$ for each trajectory according to (2). The free-energy change in the alchemical process is calculated using the usual Jarzynski equality (4) as

$$\Delta_{(ii)} F = -k_B T \log \langle e^{-\beta \hat{W}_{(ii)}} \rangle. \quad (17)$$

$\Delta_{(ii)} F$ corresponds to the free-energy change for the total system because this process does not affect the free energy of the right chamber. At constant volume, the pressure in the left chamber may be changed by process (ii) and different from that of the right chamber in general.

Before proceeding to the next process, we replace the wall partition inserted in (i) with two semi-permeable membranes. The thickness of the two membranes is the same as that of the wall partition. Assuming that the two membranes do not interact with each other, the replacement does not require thermodynamic work or affect the free energy of the system. We assume that each membrane is ideal as it does not interact with the other and allows one molecule species to pass without interaction but completely blocks the other molecule species from passing via a repulsive force.

C. Work relation for $\Delta_{(iii)} F$

Process (iii) corresponds to a standard mixing process of two pure substances, which appears in textbooks on

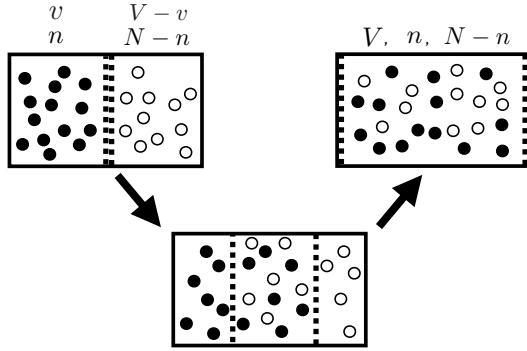


FIG. 3. Mixing process using two semipermeable membranes. $\Delta_{(iii)}F$ is calculated from the work required to shift the two semipermeable membranes.

thermodynamics [41, 42] for the demonstration of mixing entropy $\Delta_{\text{mix}}S$ and mixing free energy $\Delta_{\text{mix}}G$. Upon shifting each semi-permeable membrane slowly as shown in Fig. 3, the two substances mix together between the two membranes. When each membrane reaches the left or right boundary wall, the container is filled with the mixture of the two substances.

Before we go further, we emphasize that this mixing process makes for a difficult computation involving huge computational resources. This is because the speed of the shift of the membranes should be much lower than the velocity of molecules, whereas the distance between each membrane and each boundary wall is macroscopic. When we perform alchemical protocols such as the process in Fig. 1 and process (ii) in Fig. 2, the required time step is approximately $O(N^0)$ in calculating the work \hat{W} per trajectory. Meanwhile, process (iii) requires, at least, $O(N)$ time steps per trajectory. This number could be more, such as $O(N^2)$, because we need to relax the system close to equilibrium after each slight shift of the membranes even though we use the Jarzynski equality. Such a high-cost calculation is hard to complete with a large enough system, and this is likely the reason that process (iii) is not usually used in the numerical investigation of the mixing entropy. Only when the system is as small as $N \leq 100$ can we perform process (iii) in determining $\Delta_{(iii)}F$ with good accuracy as described below.

Suppose the work required to shift a membrane to the left boundary is $\hat{W}_{(iii)}^L(\hat{\Gamma})$ and that required to shift another membrane to the right is $\hat{W}_{(iii)}^R(\hat{\Gamma})$. The free-energy change in process (iii) is estimated to be

$$\Delta_{(iii)}F = -k_B T \log \langle e^{-\beta(\hat{W}_{(iii)}^L + \hat{W}_{(iii)}^R)} \rangle \quad (18)$$

As noticed for process (ii), the initial pressures may not be balanced between the left and right chambers in general, and therefore, process (iii) may not be quasistatic even in the thermodynamic limit. Because we are adopting the Jarzynski work relation, such problems do not

affect the estimate of the free-energy change.

D. Difference between $F_{AB\#}$ and F_{AB}

From (15), (17) and (18), we obtain

$$\Delta F = -k_B T \log \left[\rho_v(n) \langle e^{-\beta \hat{W}_{(ii)}} \rangle \langle e^{-\beta(\hat{W}_{(iii)}^L + \hat{W}_{(iii)}^R)} \rangle \right], \quad (19)$$

which is a thermodynamically valid formula for the free-energy difference (5) between the pure substance A to the mixture of A and B. We note that the left-hand side of (19) does not depend on v , whereas the respective quantities on the right-hand side are determined for a given v . Thus, the dependence on v should be canceled out by multiplying the three quantities.

Combining (19) with (7), we have

$$\beta(F_{AB} - F_{AB\#}) = -\log \frac{\rho_v(n) \langle e^{-\beta \hat{W}_{(ii)}} \rangle \langle e^{-\beta(\hat{W}_{(iii)}^L + \hat{W}_{(iii)}^R)} \rangle}{\langle e^{-\beta \hat{W}_{(\#)}} \rangle} \quad (20)$$

We emphasize that the right-hand side of (20) comprises quantities measurable in numerical thermodynamic experiments. By measuring these quantities numerically, we obtain an answer to the first question raised in Sec. III, whether $F_{AB} = F_{AB\#}$ or $F_{AB} \neq F_{AB\#}$.

E. Numerical results for the right-hand side of (20)

To obtain the right-hand side of (20), we perform molecular dynamics simulations for two types of model mixtures. One is a mixture comprising two isotopes of a monoatomic molecule, where the masses of the species A and B are set as m and $m + \Delta m$, respectively. The other is a mixture comprising monoatomic molecules that are different in size. The radius of the species A is r_0 , whereas that of B is $r_0 + \Delta r_0$. The details of the models are described in Appendix A, and the explicit protocols are specified in Appendix B. Numerical results on $\Delta_{(i)}F$, $\Delta_{(ii)}F$, and $\Delta_{(iii)}F$ are presented in Appendices C and D.

Figures 4 is a simultaneous plot of the numerical results for the right-hand side of (20) for the two mixtures. We find that all data converge to a line as

$$\log \frac{\rho_v(n) \langle e^{-\beta \hat{W}_{(ii)}} \rangle \langle e^{-\beta(\hat{W}_{(iii)}^L + \hat{W}_{(iii)}^R)} \rangle}{\langle e^{-\beta \hat{W}_{(\#)}} \rangle} = \log \frac{N!}{n!(N-n)!} \quad (21)$$

over a wide range of n/N and N for fixed V and β . The volume v for the left chamber is chosen mainly as $v = Vn/N$ as it gives the most probable value for

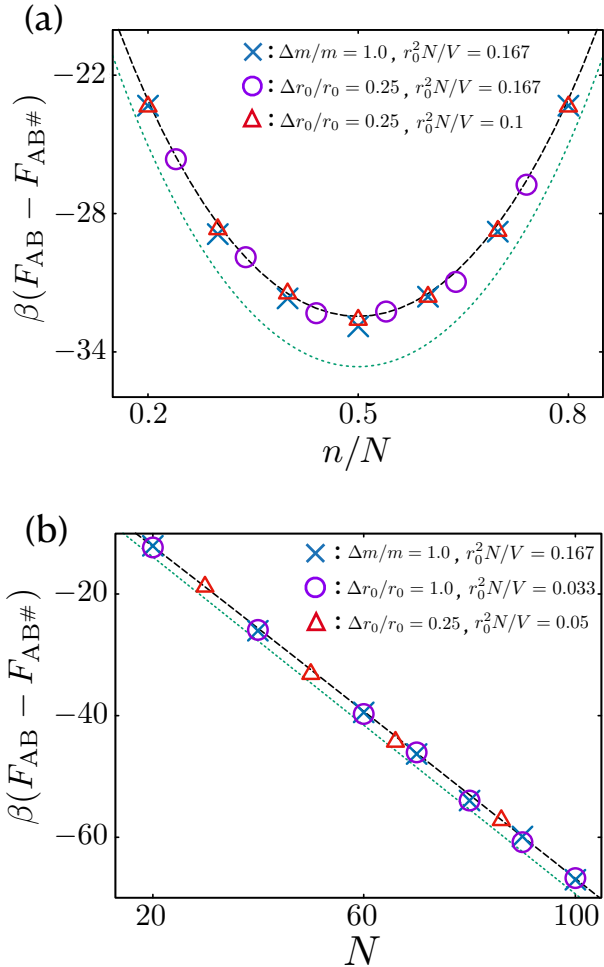


FIG. 4. $\beta(F_{AB} - F_{AB\#})$ as the right-hand side of (20) for three types of mixture: a mixture of isotopes with different masses (\times , blue) and two mixtures of two types of molecule of different size (\circ , purple and \triangle , red). The dashed black line shows $-\log[N!/n!(N-n)!]$ and the dotted green line shows $n \log n/N + (N-n) \log (N-n)/N$. (a) $\beta(F_{AB} - F_{AB\#})$ as a function of n/N for $N = 50$ with changing n and (b) $\beta(F_{AB} - F_{AB\#})$ as a function of N when $n/N = 0.5$. Error bars are not plotted as they would be smaller than the data point.

n. Combining (20) with (21), we conclude (8); i.e., $F_{AB} \neq F_{AB\#}$, and

$$\beta(F_{AB} - F_{AB\#}) = -\log \frac{N!}{n!(N-n)!}. \quad (22)$$

We emphasize that the plots in Figs. 4 contain the data for completely different mixtures and various values of $\Delta m/m$ and $\Delta r_0/r_0$. Therefore, the convergence strongly suggests the universality of the functional form (22) for $F_{AB} - F_{AB\#}$.

To examine the validity of (21), we draw a dotted line in Fig. 4 corresponding to $n \log \frac{n}{N} + (N-n) \log \frac{N-n}{N}$,

which is the main contribution of the right-hand side of (21) estimated using Stirling's formula and becomes dominant in the thermodynamic limit. The dotted line deviates obviously from the numerical results. Moreover, (21) seems to be valid even for a small system sizes of $N = 20$, where the difference in $\log N!$ from $N \log N$ is sufficiently large. We therefore conclude that $\beta(F_{AB} - F_{AB\#})$ does not behave as $n \log \frac{n}{N} + (N-n) \log \frac{N-n}{N}$ even though it is the mixing free energy for the ideal mixtures.

According to these numerical results, we conclude that (22) is a universal function. Combining (7) and (22), we obtain the Jarzynski relation (9) for alchemical processes. Once we obtain (9), we may recognize the combinatorial factor as the manifestation of the indistinguishability of molecules required by the connection with quantum mechanics. It is remarkable that this combinatorial factor is observed only from thermodynamic measurements of classical molecule systems as (21) without making any assumption related to quantum mechanics, nor statistical mechanics containing the indistinguishability of molecules. Our result suggests that one may derive the indistinguishability of molecules for classical systems by deriving the relation (21) theoretically.

V. NUMERICAL METHOD OF CALCULATING $\Delta_{\text{mix}}G$ FOR AN ISOTOPE MIXTURE

When the pressure and volume are kept constant in process (iii), we have $\Delta_{(iii)}F = \Delta_{\text{mix}}G$. Such a situation occurs for isotope mixtures as explained below, and we can calculate $\Delta_{\text{mix}}G$ from the numerical scheme to use the relation (18). This may be part of the answer to the second problem raised in Sec. III. However, we note that the calculation is rather impractical as discussed in the previous sections. We thus propose another scheme to calculate $\Delta_{\text{mix}}G$ without performing the macroscopic operations as process (iii). In this section, we concentrate on a mixture of isotopes, which is a simpler example for finding a formula for $\Delta_{\text{mix}}G$, and we then extend the method to other mixtures in the next section.

Below, we limit v as

$$v = \frac{n}{N}V, \quad (23)$$

which gives a natural choice of n corresponding to the most probable value.

A mixture of isotopes comprises two substances different only in their mass. The interaction potential $\Phi(\{r_i\})$ is common between the pure substances and the resulting mixture. The pressure p is kept constant over all processes shown in Table I while the system is at constant volume. It is thus possible to regard that all processes at constant volume are performed at constant pressure, which results in $\Delta G = \Delta F$ for all processes. Moreover, because the internal energy of the system $U = \langle H \rangle$ never changes, we have $\Delta S = -\Delta F/T$. Process (iii) then cor-

responds to a usual mixing process with

$$\Delta_{\text{mix}}G^{\text{isotope}} = \Delta_{(\text{iii})}F, \quad (24)$$

$$\Delta_{\text{mix}}S^{\text{isotope}} = -\Delta_{(\text{iii})}F/T, \quad (25)$$

where we use the superscript “isotope” to clarify the subject of the relations.

We note that the processes in Fig. 2 form a cycle once we identify the operation depicted by the red arrow, whose free-energy difference is given by (9) with the alchemical operation in Fig. 1. Thus, substituting (9), (15), and (17) into $\Delta_{(\text{iii})}F = \Delta F - \Delta_{(\text{i})}F - \Delta_{(\text{ii})}F$, we obtain the mixing Gibbs free energy for two isotopes as

$$\Delta_{\text{mix}}G^{\text{isotope}} = -k_B T \log \left[\frac{N!}{n!(N-n)! \rho_v(n)} \frac{\langle e^{-\beta \hat{W}(\#)} \rangle}{\langle e^{-\beta \hat{W}(\text{ii})} \rangle} \right]. \quad (26)$$

The right-hand side of (26) comprises numerically accessible quantities whose computational cost is much lower than the cost for performing (18).

The relation (26) is further simplified using

$$\log \rho_v(n = Nv/V) = -\frac{1}{2} \log N + o(\log N), \quad (27)$$

which is derived in Appendix C. Combining the estimate (27) with Stirling’s formula, $\log N! = N \log N - N + \frac{1}{2} \log N + o(\log N)$, we have

$$\log \frac{N!}{n!(N-n)! \rho_v(n)} = \frac{\Delta_{\text{mix}}S^{\text{id}}}{k_B} + o(\log N), \quad (28)$$

where $\Delta_{\text{mix}}S^{\text{id}}$ is the mixing entropy for ideal solutions

$$\Delta_{\text{mix}}S^{\text{id}} \equiv -k_B \left[n \log \frac{n}{N} + (N-n) \log \frac{N-n}{N} \right]. \quad (29)$$

Substituting (28) into (26), we arrive at

$$\Delta_{\text{mix}}G^{\text{isotope}} = -T \Delta_{\text{mix}}S^{\text{id}} - k_B T \log \frac{\langle e^{-\beta \hat{W}(\#)} \rangle}{\langle e^{-\beta \hat{W}(\text{ii})} \rangle} + o(\log N). \quad (30)$$

Formula (30) indicates that $\Delta_{\text{mix}}G^{\text{isotope}}$ is accessible only by the two alchemical processes. Here, we comment that, in the case of isotopes, the two ensemble averages in the second term of the right-hand side are always equal and $\Delta_{\text{mix}}G^{\text{isotope}} = -T \Delta_{\text{mix}}S^{\text{id}}$. Furthermore, because the mixing enthalpy $\Delta_{\text{mix}}H^{\text{isotope}} = 0$, we have $\Delta_{\text{mix}}S^{\text{isotope}} = \Delta_{\text{mix}}S^{\text{id}}$. Such simple relations do not hold for other mixtures, and indeed, the formula (30) provides a new method of obtaining the mixing free energy $\Delta_{\text{mix}}G$ as explained in the next section.

VI. GENERALIZATION TO REAL SOLUTIONS

We now extend the formulas (26) and (30) from the mixture of isotopes to general real solutions. In Sec.

VIA, we set up the system and its Hamiltonian at constant pressure and explain the version of the Jarzynski work relation for constant pressure. In Sec. VIB, we propose the formulas (40), (41) and (43) for $\Delta_{\text{mix}}G$ with two types of alchemical work $\hat{W}_{(\text{ii})}$ and $\hat{W}_{(\#)}$ and restate them as the relations for the activity coefficients in (48).

A. Setup at constant pressure

When a certain wall of the container is replaced with a movable wall at constant pressure of p , the system’s Hamiltonian changes to

$$H_p(\Gamma, V; \alpha) = H(\Gamma; \alpha) + pV. \quad (31)$$

Note that the pressure p is a fixed constant, whereas the volume V becomes a microscopic variable for the Hamiltonian. A trajectory in phase space is given by $(\hat{\Gamma}, \hat{V}) = (\Gamma(t), V(t))_{t \in [0, \tau]}$. When a set of parameters α is used, the required work is written as

$$\hat{W}(\hat{\Gamma}, \hat{V}) = \int_0^\tau ds \frac{d\alpha}{ds} \cdot \frac{\partial H(\Gamma(s); \alpha)}{\partial \alpha} \Big|_{\alpha=\alpha(s)}, \quad (32)$$

where \hat{W} is determined by the Hamiltonian $H(\Gamma)$ and not by $H_p(\Gamma, V)$ because the second term pV in (31) does not depend on α at fixed p . Similarly to the system at constant volume, the work in macroscopic operations or single-molecule manipulations leads to the Jarzynski work relation

$$\Delta G = -k_B T \log \langle e^{-\beta \hat{W}} \rangle, \quad (33)$$

where ΔG is the change in the Gibbs free energy $G(T, p, \alpha, N)$. $\langle \cdot \rangle$ is the average over trajectories $(\hat{\Gamma}, \hat{V})$ starting from equilibrium states at constant pressure, which corresponds to the usual ensemble average in numerical experiments starting after a sufficient relaxation.

B. Formulas for mixing free energy and activity coefficients

Following the previous argument, we consider a cycle at constant pressure shown in Fig. 5, which is similar to the cycle in Fig. 2 at constant volume.

Performing all processes at constant pressure of p , the cycle in Fig. 5 leads to

$$\Delta G = \Delta_{(\text{i})}G + \Delta_{(\text{ii})}G + \Delta_{(\text{iii})}G, \quad (34)$$

where

$$\Delta G \equiv G_{AB}(T, p, n, N-n) - G_A(T, p, N). \quad (35)$$

Operationally, ΔG is the free-energy difference due to the alchemical process that changes the pure substance of A

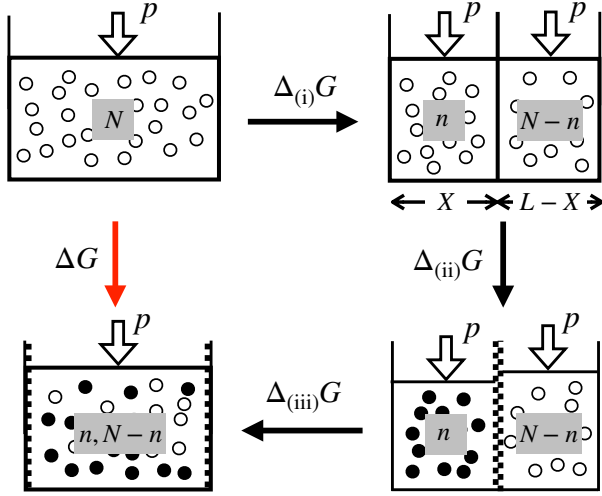


FIG. 5. Cycle at constant pressure designed in parallel to the cycle at constant volume in Fig. 2.

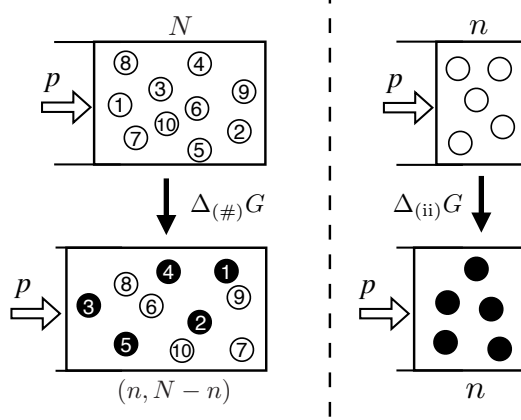


FIG. 6. Two alchemical processes to be calculated in the determination of $\Delta_{\text{mix}}G$ using formula (40), (41), or (43).

into the mixture of A and B as depicted by the red arrow in Fig. 5. Referring to formula (9), we expect that

$$\Delta G = -k_B T \log \left[\frac{N!}{n!(N-n)!} \langle e^{-\beta \hat{W}(\#)} \rangle \right], \quad (36)$$

where $\hat{W}(\#)$ is defined on the system of the distinguishable molecules according to the alchemical process illustrated in the left figure of Fig. 6.

To perform process (i) in Fig. 5, let L be the length of the container and choose X as the position to insert a wall partition. We then observe the number n in the region of $x < X$ and define $\rho_X(n)$ in parallel to (12) with the canonical distribution $\rho_{\text{eq}}(\Gamma)$ at constant pressure. The change in Gibbs free energy for process (i) is formulated

as

$$\Delta_{(i)}G = -k_B T \log \rho_X(n) \quad (37)$$

similarly to (15). The estimate (27) is also valid for the most probable value of n ; i.e., $n = NX/L$. Alchemical process (ii) at constant pressure is shown in the right figure of Fig. 6, where the right chamber is omitted. With the alchemical work $\hat{W}_{(ii)}$, the work relation (33) leads to

$$\Delta_{(ii)}G = -k_B T \log \langle e^{-\beta \hat{W}_{(ii)}} \rangle. \quad (38)$$

Protocol (iii) at constant pressure is exactly the mixing process for the two pure substances A and B; i.e.,

$$\Delta_{(iii)}G = \Delta_{\text{mix}}G. \quad (39)$$

Substituting (36), (37), (38), and (39) into (34), we have the formula for the mixing free energy as

$$\Delta_{\text{mix}}G = -k_B T \log \left[\frac{N!}{n!(N-n)!} \frac{\langle e^{-\beta \hat{W}(\#)} \rangle}{\langle e^{-\beta \hat{W}_{(ii)}} \rangle} \right]. \quad (40)$$

Obviously, formula (40) for general mixtures is consistent with (26) for isotope mixtures, and it is therefore considered to be a general work relation giving the mixing free energy $\Delta_{\text{mix}}G$. Once we obtain (40), a similar transformation from (26) to (30) is possible, which leads to

$$\Delta_{\text{mix}}G = -T \Delta_{\text{mix}}S^{\text{id}} - k_B T \log \frac{\langle e^{-\beta \hat{W}(\#)} \rangle}{\langle e^{-\beta \hat{W}_{(ii)}} \rangle} + o(\log N). \quad (41)$$

Recalling (7), the Gibbs free-energy change in the alchemical process for the distinguished molecules in the right figure of Fig. 6 is written as

$$\Delta_{(\#)}G = G_{AB\#} - G_A = -k_B T \log \langle e^{-\beta \hat{W}(\#)} \rangle. \quad (42)$$

Substituting (38) and (42) into (41), we obtain

$$\Delta_{\text{mix}}G = -T \Delta_{\text{mix}}S^{\text{id}} - \Delta_{(ii)}G + \Delta_{(\#)}G + o(\log N). \quad (43)$$

We emphasize that $\Delta_{\text{mix}}G$ is determined just from two alchemical processes in Fig. 6. Compared with the calculation of the mixing free energy along process (iii), the numerical cost to calculate (41) or (43) is low.

Mixing changes the thermodynamic properties of each substance. This change is represented by excess chemical potential; i.e., the deviation of chemical potential from that of each pure substance. Letting the concentration of the mixture be $c \equiv n/N$, the excess chemical potential is written as

$$\beta \mu_A^{\text{ex}}(T, p, c) = \log c + \log \gamma_A, \quad (44)$$

$$\beta \mu_B^{\text{ex}}(T, p, c) = \log(1 - c) + \log \gamma_B, \quad (45)$$

with the activity coefficients $\gamma_A(T, p, c)$ and $\gamma_B(T, p, c)$. When $\gamma_A = \gamma_B = 1$, the mixture is ideal; i.e., a molecule of substance A does not interact with a molecule of B. Therefore, the values of $\log \gamma_A$ and $\log \gamma_B$ represent the intrinsic properties of the mixture that result from the interaction of the two pure substances. For the total mixture, the effect of mixing is summarized by the mixing Gibbs free energy $\Delta_{\text{mix}}G$,

$$\Delta_{\text{mix}}G = n\mu_A^{\text{ex}} + (N - n)\mu_B^{\text{ex}}. \quad (46)$$

Summarizing (44), (45), and (46), we have

$$\Delta_{\text{mix}}G + T\Delta_{\text{mix}}S^{\text{id}} = k_B T [n \log \gamma_A + (N - n) \log \gamma_B]. \quad (47)$$

Thus, (41) and (43) lead to a relation for the activity coefficients as

$$\begin{aligned} n \log \gamma_A + (N - n) \log \gamma_B &= -\log \frac{\langle e^{-\beta \hat{W}_{(\#)}} \rangle}{\langle e^{-\beta \hat{W}_{(\text{ii})}} \rangle} + o(\log N) \\ &= \beta(\Delta_{(\#)}G - \Delta_{(\text{ii})}G) + o(\log N). \end{aligned} \quad (48)$$

The estimates of activity coefficients are a major issue in the research of mixtures, especially from the point of chemical engineering. The relation (48) may offer a new method of estimating the activity coefficients for various mixtures and solutions, which involves only a molecular dynamics simulation with two types of alchemical process.

VII. NUMERICAL DEMONSTRATION OF $\Delta_{\text{mix}}G$ FOR A MIXTURE OF ARGON AND KRYPTON

We present an example of $\Delta_{\text{mix}}G$ determined from the molecular dynamics simulation for a mixture of argon and krypton at constant temperature and constant pressure. The mixture is modeled as three-dimensional Lennard-Jones liquids. We use the LAMMPS package in this demonstration. See Appendix F for details. The molecules are packed in a rectangle container whose volume can fluctuate while keeping an aspect ratio of 21 : 5 : 5 to fix the value of pressure. The container is periodic in y and z directions whereas two boundary walls are set perpendicularly to the x axis.

We choose the values of temperature and pressure as $T = 163.15\text{ K}$ and $p = 4\text{ MPa}$, at which liquid-vapor transition is observed with an increasing molar fraction $c_{\text{Kr}} = N_{\text{Kr}}/N$ of the krypton [43]. The total number of molecules is $N = 500$, and the characteristics of the liquid-vapor transition are observed in numerical experiments. Figures 7 shows snapshots of the system's configuration after sufficient relaxation for $c_{\text{Kr}} = 0.3, 0.5$, and 0.65 . The volume differs greatly among the three values of c_{Kr} . The number density at $c_{\text{Kr}} = 0.65$ is approximately 5 times that at $c_{\text{Kr}} = 0.3$, and dense and dilute

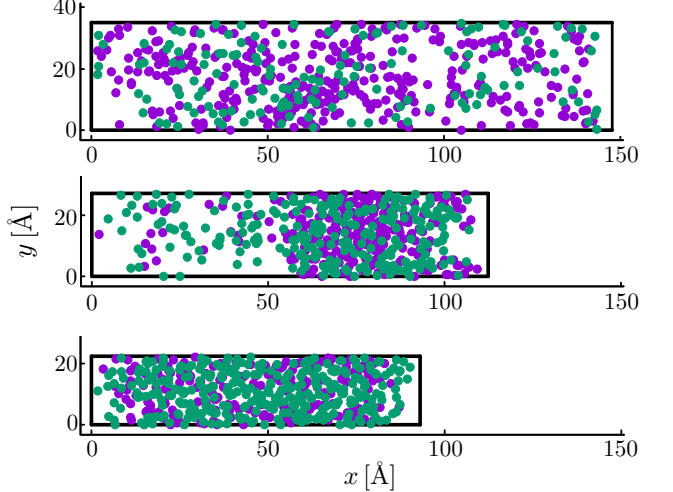


FIG. 7. Snapshots of the particle distribution for the mixture of argon (purple) and krypton (green). The three-dimensional space inside the container is projected onto the xy plane. Upper, middle, and bottom figures are for $c_{\text{Kr}} = 0.3, 0.5$, and 0.65 , respectively. The middle figure clearly shows the separation of liquid from vapor.

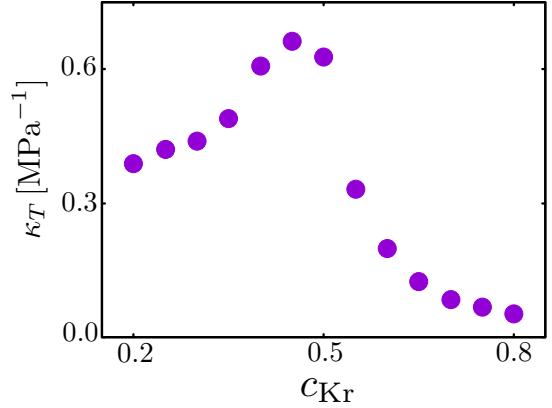


FIG. 8. Compressibility κ_T for the mixture comprising argon and krypton as a function of the molar fraction c_{Kr} of krypton.

regions coexist at $c_{\text{Kr}} = 0.5$. Such behaviors clearly exhibit the characteristics of liquid-vapor transition. We also examine the compressibility $\kappa_T \equiv -\frac{1}{\langle V \rangle} \left(\frac{\partial \langle V \rangle}{\partial p} \right)_T$, which can be written as

$$\kappa_T = \frac{\langle V^2 \rangle - \langle V \rangle^2}{k_B T \langle V \rangle}. \quad (49)$$

As shown in Fig. 8, the compressibility decreases and approaches zero when c_{Kr} is larger than 0.55, which indicates the behavior of liquid. For c_{Kr} smaller than almost 0.35, the mixture behaves as a gas, with the compressibility being larger than that of liquid. We see that the com-

pressibility grows more around $0.35 < c_{\text{Kr}} < 0.55$. This is due to the coexistence of liquid and gas, for which the volume fluctuates largely. These observations are generally consistent with the results of a previous study on argon–krypton mixtures [43].

With the above observations, we proceed to the determination of $\Delta_{\text{mix}}G$. Because the LAMMPS package does not contain the Jarzynski work relation, we calculate $\Delta_{(\#)}G$ and $\Delta_{(\text{ii})}G$ by the free-energy perturbation method [44] and substitute them into (43). In the calculations, we take the initial pure substance as being argon.

The resulting mixing free energy $\Delta_{\text{mix}}G$ is shown in Fig. 9. The curve has a double-well shape and is convex upwards in the approximate range of $0.35 < c_{\text{Kr}} < 0.55$, which is consistent with the range in which the liquid–vapor coexistence is observed in the compressibility κ_T . We thus conclude that the functional shape of $\Delta_{\text{mix}}G$ well characterizes the liquid–vapor transition for the argon–krypton mixture. Our formula, (40), (41), or (43), actually works as a quantitative method for determining the mixing Gibbs free energy.

Note that $\log N$ is 1% of N at $N = 500$ used in this demonstration, where thermodynamic properties may deviate from those in the thermodynamic limit. Indeed, the upward convexity in $\Delta_{\text{mix}}G$ is not expected in the thermodynamic limit from the second law of thermodynamics; i.e., the upward convex region should be flattened by increasing the system size N . The coexistence states may become more unstable at small N than in the thermodynamic limit owing to the enhanced fluctuations. Such finite size effects could be studied in terms of $\Delta_{\text{mix}}G$ as an interesting future topic.

VIII. CONCLUDING REMARKS

We extended the scope of the work relation from macroscopic operations or single-molecule manipulations to microscopic operations in alchemical processes, which produce a mixture from a pure substances. To this end, we numerically derived the relation (21), in which the combinatorial factor $N!/n!(N-n)!$ was led from molecular dynamics simulations for classical molecule systems. The free energy of the mixture determined by the work relation (9) or (36) is regarded as that measured in the standard reference by taking the free energy of the initial pure substance as the standard value in databases. The free energy in the standard reference makes it possible to compare thermodynamic properties among several mixtures. We then proposed a variant of the work relation for determining the mixing Gibbs free energy characterizing thermodynamic properties for the mixture. This variant is formulated as (40), (41), or (43) by combining two alchemical processes in Fig. 6 and is connected to the excess chemical potential and activity coefficients for each substance in the mixture. We demonstrated the calculation of the mixing free energy for the mixture of argon and krypton, which clearly shows the characteris-

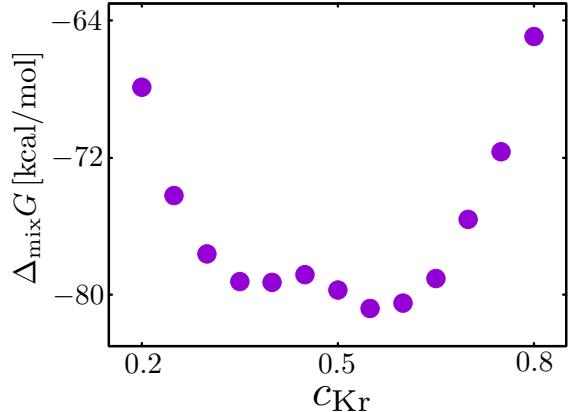


FIG. 9. $\Delta_{\text{mix}}G$ for the binary mixture of argon and krypton with $N = 500$ determined using (43). Molecular dynamics simulations are performed with a unit time of 4.0 fs. The typical relaxation time is sufficiently shorter than 1.0 ns. The alchemy operation producing the target mixture from the pure argon gas is divided into 20 steps to apply the free-energy perturbation method for the calculations of $\Delta_{(\#)}G$ and $\Delta_{(\text{ii})}G$. For each step, the system relaxes in 1.0 ns. The number of samples is 25,000.

ties of the liquid–vapor transition even in a small system of $N = 500$.

We emphasize that formulas (40), (41), and (43) offer effective methods of numerically determining the mixing free energy. The advantages of the method are the generality of the subjected mixture, accessibility to the free energy, and low cost of the numerical computation. Although we explored the method by limiting ourselves to a mixture of monoatomic molecules without electrical charges, the method would be applicable to various solutions with a general concentration, system size, species of molecules, and type of interaction. For instance, the extension of the method to diatomic or polyatomic molecules is straightforward if the number of atoms for each molecule in the mixture is the same; e.g., a mixture of O_2 and N_2 or CO_2 and H_2O . To deal with a mixture comprising two species with the different numbers of atoms, we need to take care of the indistinguishability of atoms in the molecules. We may avoid the difficulty by choosing the species of the initial pure substance as the larger molecule. We apply the alchemical process to cut the larger molecules into the same size as the smaller molecules and to change them into the target molecules. Respective alchemy tricks can be considered in accessing the mixing free energy for the respective target mixture.

Many solvation studies assume solutions to be dilute and apply the continuum limit approximation to the solvent [38]. Our method is free from such approximations and the reliability of the obtained mixing free energy depends on the reliability of the interaction potentials used, whose designs have been intensively studied for the development of molecular dynamics simulations [45]. We here

mention methods of estimating the mixing free energy and activity coefficients. For ionic solutions of less ionic strength, the Debye–Hückel theory and its extension are effective [40, 46]. For real solutions with general concentrations, heuristic approaches can be used to obtain an approximate perspective of the solutions. For instance, a method estimates activity coefficients using empirical models that require thermodynamic parameter inputs to be determined in other experiments. Another method uses approximate partition functions by imposing simpler interaction potentials with which the partition function becomes accessible [46–48]. There, the reliability of the obtained values is rather obscure owing to the heuristic assumptions.

We next remark on a fundamental point raised by the numerical experiments of this paper. Our observations revealed the combinatorial factor as shown in (21) and Fig. 4. This would be interpreted naturally as coming from the factorial $N!$ contained in the micro-canonical or canonical distribution, and may be universal over the choice of two substances. Let us recall that the factorial was initially introduced into classical statistical mechanics to satisfy the extensivity of free energy [41]. This was attributed to the indistinguishability of molecules, which was convincing owing to the consistency with quantum mechanics, although it led to the Gibbs paradox from a classical point of view. The Gibbs paradox has been argued until now as a fundamental problem; e.g., the interpretation of the distinguishability from the fluctuation theorem [49] and the ability to distinguish quantum systems [50, 51]. We emphasize that our numerical experiments reveal the combinatorial factor only from the thermodynamic measurements of classical systems without making any assumption connected to quantum mechanics. This may be related to the fact that colloidal particle systems are accessible using a framework of statistical mechanics [52]. The indistinguishability of molecules may be derived by dealing with the right-hand side of (21) theoretically for classical systems, which may shed new light on the Gibbs paradox.

Our numerical observations for isotopes with small N reveal the functional form of the mixing entropy as $n \log n/N + (N - n) \log(N - n)/N$, which is consistent with the mixing entropy for ideal mixtures derived from statistical mechanics. We here note that (28) does not only result from the combinatorial factor. It is not $\log [N!/n!(N - n)!]$ but requires the contribution of $\Delta_{(i)}F$ from information thermodynamics. Combinatorial entropic effects due to the combination may be related to the stability of binding states of two biomolecules or absorption states of small objects [53], for which the informative contribution may play a role.

Acknowledgment.— The authors thank Takenobu Nakamura for valuable comments and technical information for numerical simulation, Shin-ichi Sasa, Kyousuke Tachi, Yuya Kai, Yohei Nakayama, and Minoru Kanega for fruitful discussions. The computation in this work was done using the facilities of the Supercomputer Cen-

ter, the Institute for Solid State Physics, The University of Tokyo. The present study was supported by KAKENHI (Nos. 17H01148, 19K03647, 20K20425).

Appendix A: Model

We consider two-dimensional systems, where N molecules are in a container of a rectangle box with dimensions of $L_x \times L_y$ and a periodic boundary condition in the y direction. The position of the i th molecule, $1 \leq i \leq N$, is $\mathbf{r}_i = (x_i, y_i)$ with $0 \leq x_i \leq L_x$ and $0 \leq y_i < L_y$. Two fixed walls are placed at $(0, y)$ and (L_x, y) , and two movable membranes are at $(X_L(t), y)$ and $(X_R(t), y)$. The mass and radius of the i th molecule are m_i and r_0^i , and the thickness of each wall and membrane is σ_w . We set σ_w as almost vanishing compared with the radius of the molecules. We then define the system's Hamiltonian as

$$H(\Gamma; \alpha) = \sum_{i=1}^N \frac{|\mathbf{p}_i|^2}{2m_i} + \Phi(\{\mathbf{r}_i\}; \{r_0^i\}, X_L, X_R, \lambda), \quad (A1)$$

where λ is a parameter that denotes the existence of the inserted membranes. α is the set of parameters in the Hamiltonian; i.e.,

$$\alpha = (\{m^i\}, \{r_0^i\}, X_L, X_R, \lambda). \quad (A2)$$

We write the total potential of the system as

$$\begin{aligned} \Phi(\{\mathbf{r}_i\}; \{r_0^i\}, X_L, X_R, \lambda) = & \sum_{i=1}^N \sum_{j < i} \phi(|\mathbf{r}_i - \mathbf{r}_j|; r_0^i + r_0^j) \\ & + \sum_{i=1}^N \phi(x_i; r_0^i + \sigma_w) + \sum_{i=1}^N \phi(L_x - x_i; r_0^i + \sigma_w) \\ & + \lambda \left[\sum_{i_L=1}^n \phi(X_R - x_{i_L}; \sigma_w) + \sum_{i_R=n+1}^N \phi(x_{i_R} - X_L; \sigma_w) \right]. \end{aligned} \quad (A3)$$

All the pair interactions between two objects are given by the Weeks–Chandler–Andersen (WCA) potential,

$$\phi(r; \sigma) = \begin{cases} 4\epsilon \left[\left(\frac{\sigma}{r} \right)^{12} - \left(\frac{\sigma}{r} \right)^6 \right] + \epsilon, & (r < 2^{\frac{1}{6}}\sigma) \\ 0, & (r \geq 2^{\frac{1}{6}}\sigma) \end{cases} \quad (A4)$$

where r is the distance for the interacting pair and σ is the parameter given for respective pairs.

The first term of (A3) is the interaction between two molecules, and the second and third terms are the interactions between the molecules and walls of the container. The fourth and fifth terms of (A3) correspond to the interaction between the semipermeable membranes and molecules. i_L and i_R are the indices for labeling molecules observed in the left and right chambers, respectively. Note that the membranes detect the molecules as

points with mass. This was designed to reduce the excluded volume effect due to the insertion of the semipermeable membrane to zero.

We perform a molecular dynamics simulation with a Langevin thermostat having temperature T . Each molecule evolves according to

$$\dot{\mathbf{p}}_i = -\frac{\partial H}{\partial \mathbf{r}_i} - \frac{\gamma(x_i)}{m_i} \mathbf{p}_i + \sqrt{2\gamma(x_i)k_{\text{B}}T} \boldsymbol{\xi}_i(t), \quad (\text{A5})$$

with $\dot{\mathbf{r}}_i = \mathbf{p}_i/m_i$, where $\gamma(x_i) = 1$ in the region $0 < x_i < 0.1L_x$ and $0.9L_x < x_i < L_x$ while $\gamma(x_i) = 0$ in $0.1L_x \leq x_i \leq 0.9L_x$. $\boldsymbol{\xi}_i(t) = (\xi_i^x(t), \xi_i^y(t))$ is Gaussian white noise that satisfies $\langle \xi_i^a(t) \rangle = 0$ and $\langle \xi_i^a(t) \xi_j^b(t') \rangle = \delta_{i,j} \delta_{a,b} \delta(t-t')$, where a and b are x or y . We take $k_{\text{B}}T = 2.0\epsilon$, which is far above the Alder transition temperature.

Appendix B: Protocols and works

We take two examples of a mixture of two components. The first example is a mixture of isotopes, where the two components have distinct mass. One component is of m while another is of $m + \Delta m$. The second example is a mixture with molecules of different size, where the diameter of each component is parameterized by r_0 or $r_0 + \Delta r_0$. We take $m = 1$ and $r_0 = 2^{-1/6}$ in numerical calculations demonstrated in Appendices C and D.

We first consider the protocol to produce the mixture of distinguishable molecules. The N molecules are totally indexed from $i = 1$ to N and relaxed to equilibrium with $\lambda = 0$. In the first example, we change m with r_0 fixed as

$$m_i(t) = m + \Delta m \frac{t}{\tau_{(\#)}}, \quad (\text{B1})$$

for $1 \leq i \leq n$. $\tau_{(\#)}$ is the operation time of the protocol. According to formula (2), the work required in the change of mass m is written as

$$\hat{W}_{(\#)}^m = -\frac{\Delta m}{2\tau_{(\#)}} \sum_{i=1}^n \int_0^{\tau_{(\#)}} dt \left| \frac{\mathbf{p}_i(t)}{m(t)} \right|^2. \quad (\text{B2})$$

We can take $\tau_{(\#)}$ as being very short and even $\tau_{(\#)} \rightarrow 0$ when we use the Jarzynski relation (4). In the second example, we change r_0 for the molecules with m fixed as

$$r_0^i(t) = r_0^i + \Delta r_0 \frac{t}{\tau_{(\#)}}, \quad (\text{B3})$$

where $1 \leq i \leq n$. The required work is

$$\hat{W}_{(\#)}^{r_0} = \frac{\Delta r_0}{\tau_{(\#)}} \sum_{i=1}^n \int_0^{\tau_{(\#)}} dt \left. \frac{\partial \Phi(\{\mathbf{r}_i(t)\}; \{r_0^i\}, 0, 1, 0)}{\partial r_0^i} \right|_{\{r_0^i\} = \{r_0^i(t)\}}. \quad (\text{B4})$$

When we consider a dilute fluid, we can take the period of operation as $\tau_{(\#)} \rightarrow 0$.

We next describe the protocol used to determine $\Delta_{(\text{i})}F$, $\Delta_{(\text{ii})}F$ and $\Delta_{(\text{iii})}F$. For process (i), we put N molecules in the container with $\lambda = 0$ and relax the system in equilibrium. At each moment t after the relaxation, we observe the number of the molecules $n_v(\Gamma(t))$ in the region corresponding to the left chamber; i.e., $x < v/L_y$. From this observation, we construct the probability density $\rho_v(n)$. We then obtain $\Delta_{(\text{i})}F$ according to (15).

In process (ii), we deal with the system with $\lambda = 1$ as it is separated by the wall. We choose an arbitrary value of n and put n molecules in the left chamber having volume v , and $N - n$ molecules in the right chamber having volume $V - v$. In this paper, we choose $n = Nv/V$ because the left and right systems become almost equivalent. We label molecules in the left and right chambers as i_{L} and i_{R} , respectively, where $1 \leq i_{\text{L}} \leq n$ and $n + 1 \leq i_{\text{R}} \leq N$. We relax this combined system to equilibrium. Note that the procedures up to here are common for all mixtures that we want to examine. We then start alchemical process (ii). In the first example, we set the initial mass of all molecules as $m_i = m$. We change the mass of the left n molecules while fixing that of the right molecules as

$$m_{i_{\text{L}}}(t) = m + \Delta m \frac{t}{\tau_{(\text{ii})}}, \quad m_{i_{\text{R}}}(t) = m, \quad (\text{B5})$$

for $0 \leq t \leq \tau_{(\text{ii})}$. In $t \geq \tau_{(\text{ii})}$, the masses are fixed as $m + \Delta m$ and m in left and right chambers, respectively. The work required for this change is

$$\hat{W}_{(\text{ii})}^m = -\frac{\Delta m}{2\tau_{(\text{ii})}} \sum_{i_{\text{L}}=1}^n \int_0^{\tau_{(\text{ii})}} dt \left| \frac{\mathbf{p}_{i_{\text{L}}}(t)}{m_{i_{\text{L}}}(t)} \right|^2. \quad (\text{B6})$$

In the second example, we set the initial radius of all molecules as r_0 and then change the radius in the left chamber as

$$r_0^{i_{\text{L}}}(t) = r_0 + \Delta r_0 \frac{t}{\tau_{(\text{ii})}}, \quad r_0^{i_{\text{R}}}(t) = r_0, \quad (\text{B7})$$

for $0 \leq t \leq \tau_{(\text{ii})}$, and then fix the radii. The required work is

$$\hat{W}_{(\text{ii})}^{r_0} = \frac{\Delta r_0}{\tau_{(\text{ii})}} \sum_{i_{\text{L}}=1}^n \int_0^{\tau_{(\text{ii})}} dt \left. \frac{\partial \Phi(\{\mathbf{r}_i(t)\}; \{r_0^i\}, \frac{v}{L_y}, \frac{v}{L_y}, 1)}{\partial r_0^{i_{\text{L}}}} \right|_{\{r_0^i\} = \{r_0^i(t)\}}. \quad (\text{B8})$$

We equilibrate the system for an interval t_{r} sufficiently longer than the system's relaxation time. We then proceed to protocol (iii), which is the hardest process in the computation. Note that the pressure will be different between the left and the right chambers, especially in the second example. Such a difference may be a cause of irreversibility; however, this does not matter in principle for the use of the Jarzynski work relation.

We start to move the two membranes at time $t_1 = \tau_{(ii)} + t_r$, which is expressed as

$$X_L(t) = \frac{v}{L_y} \left(1 - \frac{t - t_1}{\tau_{(iii)}} \right), \quad (B9)$$

$$X_R(t) = \frac{V}{L_y} - \frac{V - v}{L_y} \left(1 - \frac{t - t_1}{\tau_{(iii)}} \right) \quad (B10)$$

for $t_1 < t < t_1 + \tau_{(iii)}$, in which the operation time $\tau_{(iii)}$ is as long as

$$\tau_{(iii)} \sim \max \left(\frac{v}{r_0^{i_L}(t_1)}, \frac{V - v}{r_0^{i_R}} \right) \quad (B11)$$

to avoid numerical errors and/or divergence. The works along this protocol are

$$\hat{W}_{(iii)}^L = -\frac{v}{L_y} \frac{1}{\tau_{(iii)}} \int_{t_1}^{t_1 + \tau_{(iii)}} dt \left. \frac{\partial \Phi(\{r_i(t)\}; \{r_0^i(t_1)\}, X_L, X_R(t), 1)}{\partial X_L} \right|_{X_L=X_L(t)} \quad (B12)$$

and

$$\hat{W}_{(iii)}^R = \frac{V - v}{L_y} \frac{1}{\tau_{(iii)}} \int_{t_1}^{t_1 + \tau_{(iii)}} dt \left. \frac{\partial \Phi(\{r_i(t)\}; \{r_0^i(t_1)\}, X_L(t), X_R, 1)}{\partial X_R} \right|_{X_R=X_R(t)} \quad (B13)$$

Appendix C: General estimate of $\Delta_{(i)}F$

Figure 10(a) shows an example of the distribution $\rho_v(n)$ for $v = V/2$ when $N = 50$. It clearly shows that $\rho_v(n)$ is approximated well by a Gaussian distribution exhibited by a line. We calculate $\Delta_{(i)}F$ by (15) from numerically determined $\rho_v(\langle n \rangle)$. As shown in Fig. 10(b) for $20 \leq N \leq 100$, $\Delta_{(i)}F$ exhibits a logarithm of N , which will be common over species of the initial substance, as explained below.

Once we choose the values of v , V , and N , we naturally expect the mean number of the molecules in the left chamber to be $\langle n \rangle = Nv/V$. We here assume $v = O(V)$ and $V - v = O(V)$. The probability distribution $\rho_v(n)$ is generally written as

$$\rho_v(n) = \frac{1}{C_v(N)} \exp \left[-N \sum_{k=2}^{\infty} \frac{a_k}{k!} \left(\frac{n}{N} - \frac{\langle n \rangle}{N} \right)^k \right], \quad (C1)$$

$$C_v(N) = N \int_0^1 dc \exp \left[-N \sum_{k=2}^{\infty} \frac{a_k}{k!} (c - \langle c \rangle)^k \right], \quad (C2)$$

where a_k is a constant of $O(N^0)$ and $c = n/N$. Substituting $n = \langle n \rangle$ into the above general form, we have

$$\log \rho_v(\langle n \rangle) = -\log C_v(N). \quad (C3)$$

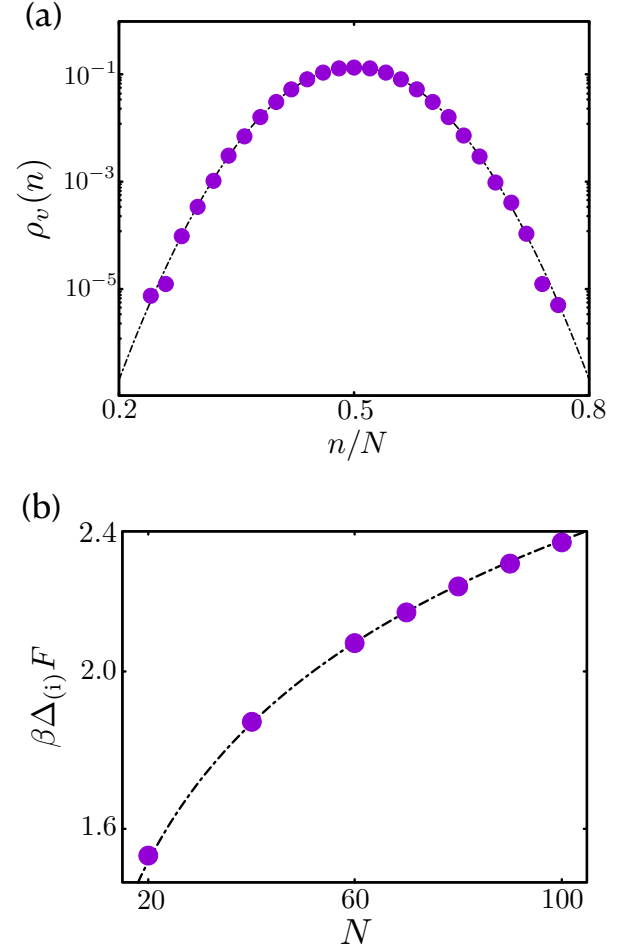


FIG. 10. (a) Distribution of the number of molecules $\rho_v(n)$ for $N = 50$. The line indicates the Gaussian distribution with $\langle n \rangle = N/2$ and $\sigma(n) = 0.42\sqrt{N}$. (b) $\Delta_{(i)}F$ resulting from the numerically determined $\rho_v(n)$ at $n = Nv/V$ for $20 \leq N \leq 100$. The line indicates $\beta\Delta_{(i)}F = \frac{1}{2} \log N$ as (C6). To obtain each point, $\rho_v(n = Nv/V)$ is determined from 50,000 samples for $V = 30Nr_0^i$ and $v = V/2$ in both (a) and (b).

A standard procedure for large N leads to an estimate as

$$C_v(N) = \sqrt{N} \left(\sqrt{\frac{2\pi}{a_2}} + o(N^{-\frac{1}{2}}) \right), \quad (C4)$$

which yields

$$\log \rho_v(\langle n \rangle) = -\frac{1}{2} \log N + o(\log N). \quad (C5)$$

Therefore, especially for $n = \langle n \rangle = Nv/V$, (15) is rewritten as

$$\beta\Delta_{(i)}F = \frac{1}{2} \log N + o(\log N) \quad (C6)$$

from (C5). Note that this formula holds universally for any mixture. The numerical results are presented in

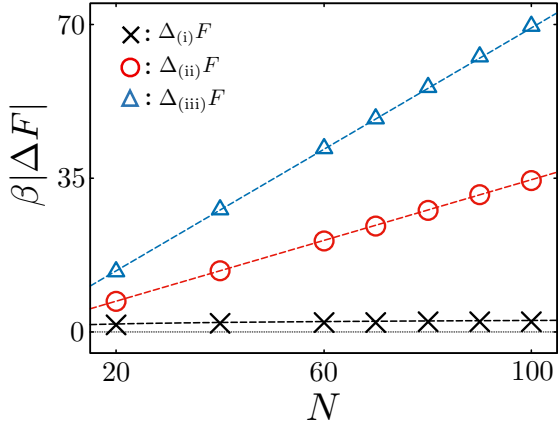


FIG. 11. Free-energy changes $\Delta_{(i)}F$, $\Delta_{(ii)}F$, and $\Delta_{(iii)}F$ for the change in mass $m \rightarrow 2m$ as a function of N . The volume v for the left chamber is chosen as $v = Vn/N$, where $V = 6Nr_0^2$ and $n/N = 0.5$. Lines are estimates of (D4), (D5), and (D6) from statistical mechanics.

process	a	b	operation time
(ii)	-0.346 ± 0.001	0.003 ± 0.018	$400\tau_{\text{MD}}$
(iii)	-0.700 ± 0.001	0.069 ± 0.019	$30000\tau_{\text{MD}}$
(#)	-0.349 ± 0.005	0.033 ± 0.010	$400\tau_{\text{MD}}$

TABLE II. Values of fitting parameters a and b in (D3) when changing the mass as $m \rightarrow 2m$ for n molecules. $n = 0.5N$, $V = 6Nr_0^2$ and $v = 0.5V$. Operation times $\tau_{(ii)}$ and $\tau_{(iii)}$ are depicted in the last columns.

Fig. 10(b), which shows a good agreement with (C6) depicted as a line.

Appendix D: Numerical results on respective free-energy changes

We here demonstrate numerical estimates of respective free-energy changes to clarify their N dependence.

We focus on small values of N as $N \leq 100$, where $\log N!$ largely deviates from $N \log N$. The difference is estimated using Stirling's formula as

$$\log N! - N \log N = -N + \frac{1}{2} \log N + o(\log N). \quad (\text{D1})$$

From this formula with $n = O(N)$, we have

$$\begin{aligned} \log \frac{N!}{n!(N-n)!} - \left[n \log \frac{n}{N} - (N-n) \log \frac{N-n}{N} \right] \\ = \frac{1}{2} \log \frac{N}{n(N-n)} + o(\log N), \end{aligned} \quad (\text{D2})$$

whose right-hand side is $O(\log N)$ and ignored at sufficiently large N . This indicates that identifying the

contribution of $O(\log N)$ for each free-energy difference makes the finite size effect on N clear. We therefore make numerical estimates up to $O(\log N)$ for each free-energy difference. We fit the numerical results in the functional form as

$$\beta\Delta_{(ii,iii,\#)}F = aN + b \log N, \quad (\text{D3})$$

where the first term on the right-hand side corresponds to the extensive contribution remaining in the thermodynamic limit. The second term is important to the purpose of this paper.

For numerical estimates of $\Delta_{(ii)}F$ and $\Delta_{(iii)}F$, we choose $n/N = v/V = 0.5$ and set $V = 6Nr_0^2$ for the mixture of isotopes, whereas $V = 30Nr_0^2$ for the mixture of the different size molecules. We calculate 5000 samples for each protocol.

Figure 11 shows the respective free-energy changes in the protocol $m \rightarrow 2m$, where the mixture comprises isotopes. The operation times are $\tau_{(ii)} = 400\tau_{\text{MD}}$ and $\tau_{(iii)} = 30000\tau_{\text{MD}}$, where $\tau_{\text{MD}} \equiv 2r_0\sqrt{m/\epsilon}$. As seen, both $\Delta_{(ii)}F$ and $\Delta_{(iii)}F$ increase linearly with N , which become far superior to $\Delta_{(i)}F$ at $N = 100$. The fitting parameters a and b are summarized in Table II. We find that the coefficient b is sufficiently small to ignore the contribution of $O(\log N)$. Thus, the contribution of $O(\log N)$ in ΔF comes only from $\Delta_{(i)}F$, which indicates the importance of $\Delta_{(i)}F$ to estimate free energy in the finite-size systems.

When the isotopes are an ideal gas, we can directly calculate the respective free-energy change using statistical mechanics. We derive in Appendix E

$$\beta\Delta_{(i)}F = \frac{1}{2} \log N + o(\log N), \quad (\text{D4})$$

$$\beta\Delta_{(ii)}F = -\frac{N}{2} \log 2 + o(\log N), \quad (\text{D5})$$

$$\beta\Delta_{(iii)}F = -N \log 2 + o(\log N). \quad (\text{D6})$$

We show these estimates as the lines in Fig. 11. Even though we adopt a finite radius with $r_0 \neq 0$, numerical results fit well to these theoretical results for the ideal isotopes.

Figure 12 displays numerical results for the protocol $r_0 \rightarrow 2r_0$. We remark $\Delta_{(ii)}F \neq \Delta_{(\#)}F$ as demonstrated in Table III. This is an important difference from the isotopes with $\Delta_{(ii)}F = \Delta_{(\#)}F$. The difference between $\Delta_{(ii)}F$ and $\Delta_{(\#)}F$ may indicate that the deviation of the mixture from the ideal one and characterize the nontrivial thermodynamic properties of the mixture.

Appendix E: Free-energy changes for ideal solutions of isotopes derived from statistical mechanics

The free energy for the solution of two ideal isotopes can be calculated theoretically according to statistical mechanics. The partition function for pure substance A

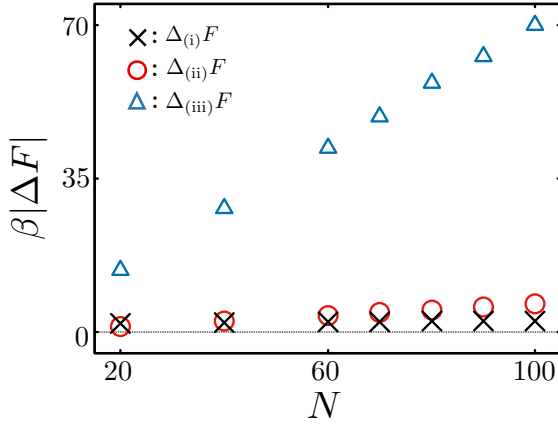


FIG. 12. Free-energy changes $\Delta_{(i)}F$, $\Delta_{(ii)}F$, and $\Delta_{(iii)}F$ for the change in radius $r_0 \rightarrow 2r_0$ as a function of N . The volume v for the left chamber is chosen as $v = Vn/N$, where $V = 30Nr_0^2$ and $n/N = 0.5$.

process	a	b	operation time
(ii)	0.066 ± 0.001	-0.060 ± 0.004	$2050\tau_{\text{MD}}$
(iii)	-0.700 ± 0.007	-0.046 ± 0.120	$15000\tau_{\text{MD}}$
(#)	$0.058(6) \pm 0.000(1)$	-0.040 ± 0.002	$2050\tau_{\text{MD}}$

TABLE III. Values of fitting parameters a and b in (D3) when changing the radius as $r_0 \rightarrow 2r_0$ for n molecules. $n = 0.5N$, $V = 6Nr_0^2$ and $v = 0.5V$. Operation times $\tau_{(ii)}$ and $\tau_{(iii)}$ are depicted in the last columns.

or B is calculated as

$$Z_A(V, N) = \frac{(2\pi k_B T m V)^N}{N!}, \quad (\text{E1})$$

$$Z_B(V, N) = \frac{(2\pi k_B T (m + \Delta m) V)^N}{N!}, \quad (\text{E2})$$

whereas that of the mixture of A and B is

$$Z_{AB}(V, n, N - n) = \frac{(2\pi k_B T V)^N m^n (m + \Delta m)^{N-n}}{n!(N-n)!}. \quad (\text{E3})$$

Since $\beta F = -\log Z$, we have the respective differences of the free energy as

$$\beta \Delta F = -n \log \frac{m + \Delta m}{m} - \log \frac{N!}{n!(N-n)!}, \quad (\text{E4})$$

$$\beta \Delta_{(ii)}F = -n \log \frac{m + \Delta m}{m}, \quad (\text{E5})$$

$$\beta \Delta_{(iii)}F = n \log \frac{n}{N} + (N - n) \log \frac{N - n}{N}. \quad (\text{E6})$$

Note that the right-hand side of (E6) is nothing but the mixing entropy for the ideal solution $-k_B \Delta_{\text{mix}} S^{\text{id}}$. This is because process (iii) for the isotope mixture does not change the internal energy and pressure of the system, which leads to $\Delta_{(iii)}F = -T \Delta_{\text{mix}} S^{\text{id}}$.

Recalling that $\Delta_{(i)}F = \Delta F - \Delta_{(ii)}F - \Delta_{(iii)}F$, (E4), (E5), and (E6) yield

$$\beta \Delta_{(i)}F = -\log \frac{N!}{n!(N-n)!} - n \log \frac{n}{N} - (N - n) \log \frac{N - n}{N}. \quad (\text{E7})$$

(E7) agrees with the estimate (27) or (C5). Applying Stirling's formula to (E7), we obtain

$$\beta \Delta_{(i)}F = \frac{1}{2} \log N + \frac{1}{2} \log \frac{2\pi n(N-n)}{N^2} + o(N^0). \quad (\text{E8})$$

This is consistent with (27) because the second term of the right-hand side is $o(\log N)$ when n/N and $(N-n)/N$ are $O(N^0)$.

Let us calculate $\Delta_{(i)}F$ directly. The probability that one molecule of ideal gas exists in a region of volume v is v/V , and the probability of finding n molecules in the region of volume v is thus given by a binomial distribution,

$$\rho_v(n) = \left(\frac{v}{V} \right)^n \left(\frac{V-v}{V} \right)^{N-n} \frac{N!}{n!(N-n)!}. \quad (\text{E9})$$

Substituting this form of $\rho_v(n)$ with $n = Nv/V$ into (15), we obtain (E7). This agreement convinces us of the validity of (15) as the formula of $\Delta_{(i)}F$.

Appendix F: Model for the mixture of argon and krypton

The interaction of any two molecules, argon or krypton, is given by the Lennard–Jones potential,

$$\phi(r; \epsilon, \sigma) = \begin{cases} 4\epsilon \left[\left(\frac{\sigma}{r} \right)^{12} - \left(\frac{\sigma}{r} \right)^6 \right], & (r < r_c) \\ 0, & (r \geq r_c) \end{cases} \quad (\text{F1})$$

where r_c is the cutoff length. The parameters of ϕ are set as reported in [54]; for the argon pair, $\sigma_{\text{Ar}} = 3.401 \text{ \AA}$ and $\epsilon_{\text{Ar}} = 0.2321 \text{ kcal/mol}$, whereas $\sigma_{\text{Kr}} = 3.601 \text{ \AA}$, $\epsilon_{\text{Kr}} = 0.3270 \text{ kcal/mol}$ for the krypton pair. For the pair of argon and krypton, the Lorentz–Berthelot law is assumed as is usual for the Lennard–Jones binary mixture [55, 56], $\sigma_{\text{ArKr}} = (\sigma_{\text{Ar}} + \sigma_{\text{Kr}})/2 = 3.501 \text{ \AA}$ and $\epsilon_{\text{ArKr}} = \sqrt{\epsilon_{\text{Ar}} \epsilon_{\text{Kr}}} 0.2755 \text{ kcal/mol}$. We set the cutoff length as $r_c = 3\sigma_{\text{Kr}}$. The masses of argon and krypton are $m_{\text{Ar}} = 39.95 \text{ g/mol}$ and $m_{\text{Kr}} = 83.80 \text{ g/mol}$.

The molecules are packed in a rectangular container, which is periodic in y and z directions whereas two soft-core walls with $\sigma_w = \sigma_{\text{Ar}}/2$ are set as they are perpendicular to the x axis. The aspect ratio of the container is kept at 21 : 5 : 5.

The numerical simulation is performed at constant temperature and constant pressure using the LAMMPS molecular dynamics package. The temperature and pressure are controlled by the Nose–Hoover chain and Martyna–Tobias–Klein barostat, respectively [57].

[1] G. M. Barrow, *Physical Chemistry*, 6th ed. (McGraw-Hill College, New Delhi, 1996).

[2] L. D. Landau and E. M. Lifshitz, *Course of theoretical physics. 5,1 Statistical physics*, 3rd ed. (Butterworth-Heinemann, Oxford, 1980).

[3] NIST Chemistry WebBook, SRD69. <https://webbook.nist.gov/chemistry/>.

[4] S. Yu, S. Wang, M. Lu, and L. Zuo, “Review of MEMS differential scanning calorimetry for biomolecular study,” *Front. Mech. Eng.* **12**, 526–538 (2017).

[5] T. Harada and S.-i. Sasa, “Equality connecting energy dissipation with a violation of the fluctuation-response relation,” *Phys. Rev. Lett.* **95**, 130602 (2005).

[6] S. Toyabe, T. Watanabe-Nakayama, T. Okamoto, S. Kudo, and E. Muneyuki, “Thermodynamic efficiency and mechanochemical coupling of F 1-ATPase,” *Proc. Natl. Acad. Sci. U. S. A.* **108**, 17951–17956 (2011).

[7] T. Ariga, M. Tomishige, and D. Mizuno, “Nonequilibrium Energetics of Molecular Motor Kinesin,” *Phys. Rev. Lett.* **121**, 218101 (2018).

[8] M. S. Cheung, D. Klimov, and D. Thirumalai, “Molecular crowding enhances native state stability and refolding rates of globular proteins,” *Proc. Natl. Acad. Sci. U. S. A.* **102**, 4753–4758 (2005).

[9] T. M. Squires and T. G. Mason, “Fluid mechanics of microrheology,” *Annu. Rev. Fluid Mech.*, *Annu. Rev. Fluid Mech.* **42**, 413–438 (2010).

[10] B. Wang, J. Kuo, S. Chul Bae, and S. Granick, “When Brownian diffusion is not Gaussian,” *Nat. Mater.*, *Nat. Mater.* **11**, 481–485 (2012).

[11] M. V. Chubynsky and G. W. Slater, “Diffusing diffusivity: A model for anomalous, yet Brownian, diffusion,” *Phys. Rev. Lett.* **113**, 098302 (2014).

[12] S. Kroschwitz and S. Alberti, “Gel or Die: Phase Separation as a Survival Strategy,” *Cell* **168**, 947–948 (2017).

[13] V. N. Uversky, “Intrinsically disordered proteins in overcrowded milie: Membrane-less organelles, phase separation, and intrinsic disorder,” *Curr. Opin. Struct. Biol.*, **44**, 18–30 (2017).

[14] E. Dolgin, “What lava lamps and vinaigrette can teach us about cell biology,” *Nature* **555**, 300–302 (2018).

[15] T. M. Franzmann, M. Jahnel, A. Pozniakovsky, J. M. Hamid, A. S. Holehouse, E. Nüske, D. Richter, W. Baumeister, S. W. Grill, R. V. Pappu, A. A. Hyman, and S. Alberti, “Phase separation of a yeast prion protein promotes cellular fitness,” *Science* **359**, eaao5654 (2018).

[16] B. Bolognesi, A. J. Faure, M. Seuma, J. M. Schmiedel, G. Gaetano Tartaglia, and B. Lehner, “The mutational landscape of a prion-like domain,” *Nat. Commun.* **10**, 1–12 (2019).

[17] S. Alberti and D. Dormann, “Liquid-Liquid Phase Separation in Disease,” *Annu. Rev. Genet.* **53**, 171–194 (2019).

[18] T. L. Hill, “Thermodynamics of Small Systems,” *J. Chem. Phys.* **36**, 3182 (1962).

[19] U. Seifert, “Stochastic thermodynamics, fluctuation theorems and molecular machines,” *Rep. Prog. Phys.* **75**, 126001 (2012).

[20] D. J. Evans, E. G.D. Cohen, and G. P. Morriss, “Probability of second law violations in shearing steady states,” *Phys. Rev. Lett.* **71**, 2401–2404 (1993).

[21] C. Jarzynski, “Nonequilibrium equality for free energy differences,” *Phys. Rev. Lett.* **78**, 2690–2693 (1997).

[22] G. E. Crooks, “Path-ensemble averages in systems driven far from equilibrium,” *Phys. Rev. E* **61**, 2361–2366 (2000).

[23] T. Sagawa and M. Ueda, “Generalized Jarzynski equality under nonequilibrium feedback control,” *Phys. Rev. Lett.* **104**, 090602 (2010).

[24] J. M.R. Parrondo, J. M. Horowitz, and T. Sagawa, “Thermodynamics of information,” *Nat. Phys.* **11**, 131–139 (2015).

[25] S. Ito and T. Sagawa, “Maxwell’s demon in biochemical signal transduction with feedback loop,” *Nat. Commun.* **6**, 1–6 (2015).

[26] C. Chipot and A. Pohorille, eds., *Free Energy Calculations: Theory and Applications in Chemistry and Physics*, Springer Series in Chemical Physics, Vol. 86 (Springer-Verlag, Berlin, 2007).

[27] B. Cheng and M. Ceriotti, “Computing the absolute Gibbs free energy in atomistic simulations: Applications to defects in solids,” *Phys. Rev. B* **97**, 054102 (2018).

[28] S. B. Smith, Y. Cui, and C. Bustamante, “Overstretching B-DNA: The elastic response of individual double-stranded and single-stranded DNA molecules,” *Science* **271**, 795–799 (1996).

[29] D. Collin, F. Ritort, C. Jarzynski, S. B. Smith, I. Tinoco, and C. Bustamante, “Verification of the Crooks fluctuation theorem and recovery of RNA folding free energies,” *Nature* **437**, 231–234 (2005).

[30] P. Kollman, “Free Energy Calculations: Applications to Chemical and Biochemical Phenomena,” *Chem. Rev.* **93**, 2395–2417 (1993).

[31] P. A. Kollman, “Advances and Continuing Challenges in Achieving Realistic and Predictive Simulations of the Properties of Organic and Biological Molecules,” *Acc. Chem. Res.* **29**, 461–469 (1996).

[32] T. Simonson, G. Archontis, and M. Karplus, “Free energy simulations come of age: Protein-ligand recognition,” *Acc. Chem. Res.* **35**, 430–437 (2002).

[33] D. L. Mobley, J. D. Chodera, and K. A. Dill, “On the use of orientational restraints and symmetry corrections in alchemical free energy calculations,” *J. Chem. Phys.* **125**, 084902 (2006).

[34] D. L. Mobley and P. V. Klimovich, “Perspective: Alchemical free energy calculations for drug discovery,” *J. Chem. Phys.*, **137**, 230901 (2012).

[35] T. Steinbrecher, C. Zhu, L. Wang, R. Abel, C. Ne Gron, D. Pearlman, E. Feyfant, J. Duan, and W. Sherman, “Predicting the Effect of Amino Acid Single-Point Mutations on Protein Stability—Large-Scale Validation of MD-Based Relative Free Energy Calculations,” *J. Mol. Biol.* **429**, 948–963 (2017).

[36] M. Kuhn, S. Firth-Clark, P. Tosco, A. S.J.S. Mey, M. MacKey, and J. Michel, “Assessment of Binding Affinity via Alchemical Free-Energy Calculations,” *J. Chem. Inf. Model.* **60**, 3120–3130 (2020).

[37] J. Scheen, W. Wu, A. S.J.S. Mey, P. Tosco, M. Mackey, and J. Michel, “Hybrid alchemical free Energy/Machine-Learning methodology for the computation of hydration free energies,”

J. Chem. Inf. Model. **60**, 5331–5339 (2020).

[38] R. E. Skyner, J. L. McDonagh, C. R. Groom, T. Van Mourik, and J. B.O. Mitchell, “A review of methods for the calculation of solution free energies and the modelling of systems in solution,” Phys. Chem. Chem. Phys. **17**, 6174–6191 (2015).

[39] M. Kohns, S. Reiser, M. Horsch, and H. Hasse, “Solvent activity in electrolyte solutions from molecular simulation of the osmotic pressure,” J. Chem. Phys. **144**, 084112 (2016).

[40] P. Debye and E. Hückel, “Zur theorie der elektrolyte. i. gefrierpunktserniedrigung und verwandte erscheinungen,” Physik. Z. **25**, 305 (1924).

[41] J. W. Gibbs, “On the equilibrium of heterogeneous substances,” Trans. Conn. Acad. Arts Sci **3**, 343–524 (1875–1878).

[42] E. Fermi, *Thermodynamics* (Dover, New York, 1956).

[43] A. E. Nasrabad, R. Laghaei, and U. K. Deiters, “Prediction of the thermophysical properties of pure neon, pure argon, and the binary mixtures neon-argon and argon-krypton by Monte Carlo simulation using ab initio potentials,” J. Chem. Phys. **121**, 6423–6434 (2004).

[44] R. W. Zwanzig, “High Temperature Equation of State by a Perturbation Method. I. Nonpolar Gases,” J. Chem. Phys. **22**, 1420–1426 (1954).

[45] H. Sun, “Compass: An ab initio force-field optimized for condensed-phase applications - Overview with details on alkane and benzene compounds,” J. Phys. Chem. B **102**, 7338–7364 (1998).

[46] C. W. Davies, “397. The extent of dissociation of salts in water. Part VIII. An equation for the mean ionic activity coefficient of an electrolyte in water, and a revision of the dissociation constants of some sulphates,” J. Chem. Soc. , 2093–2098 (1938).

[47] A. Fredenslund, R. L. Jones, and J. M. Prausnitz, “Group-contribution estimation of activity coefficients in nonideal liquid mixtures,” AIChE J. **21**, 1086–1099 (1975).

[48] A. Klamt, “Conductor-like screening model for real solvents: A new approach to the quantitative calculation of solvation phenomena,” J. Phys. Chem. **99**, 2224–2235 (1995).

[49] Y. Murashita and M. Ueda, “Gibbs Paradox Revisited from the Fluctuation Theorem with Absolute Irreversibility,” Phys. Rev. Lett. **118**, 060601 (2017).

[50] Z. Holmes, F. Mintert, and J. Anders, “Gibbs mixing of partially distinguishable photons with a polarising beam-splitter membrane,” New J. Phys. **22**, 113015 (2020).

[51] B. Yadin, B. Morris, and G. Adesso, “Mixing indistinguishable systems leads to a quantum Gibbs paradox,” Nat. Commun. **12**, 1–10 (2021).

[52] P. B. Warren, “Combinatorial entropy and the statistical mechanics of polydispersity,” Phys. Rev. Lett. **80**, 1369–1372 (1998).

[53] M. Liu, A. Apriceno, M. Sipin, E. Scarpa, L. Rodriguez-Arco, A. Poma, G. Marchello, G. Battaglia, and S. Angioletti-Uberti, “Combinatorial entropy behaviour leads to range selective binding in ligand-receptor interactions,” Nat. Commun. **11**, 1–10 (2020).

[54] S. K. Oh, “Modified Lennard-Jones potentials with a reduced temperature-correction parameter for calculating thermodynamic and transport properties: Noble gases and their mixtures (He, Ne, Ar, Kr, and Xe),” J. Thermodyn. **1**, 29 (2013).

[55] H. A. Lorentz, “Ueber die Anwendung des Satzes vom Virial in der kinetischen Theorie der Gase,” Ann. Phys. **248**, 127–136 (1881).

[56] D. Berthelot, “Sur le mélange des gaz.” Comptes Rendus de l’Academie des Sciences Paris **126**, 1703–1706 (1889).

[57] G. J. Martyna, D. J. Tobias, and M. L. Klein, “Constant pressure molecular dynamics algorithms,” J. Chem. Phys. **101**, 4177–4189 (1994).